



Computational Modelling of Lung Cancer Treats with Lupeol

Thanaraj Baskaran^a, Dhandayuthapani Kandavel^a, Vengadesan Aravindh^b, Marimuthu Koperuncholan^{b*}

^aDepartment of Botany, Thanthai Periyar Government Arts and Science College (Autonomous), Bharathidasan University, Tiruchirappalli, Tamil Nadu -620 023, India.

^bDepartment of Botany, Srimad Andavan Arts and Science College (Autonomous), Affiliated to Bharathidasan University, Tiruchirappalli, Tamil Nadu - 620 005, India.

*Corresponding author's Email: kingchola85@gmail.com

ABSTRACT

Lung cancer is one of the most common cancers worldwide, with a high fatality rate. One of the most efficient methods for discovering medications for critical diseases is molecular docking. The crystal structures of CPd8 and Lupeol were used in the MD simulation. The data were examined, and the interactions between the protein and the ligand were confirmed in several ways before the greatest binding affinity was chosen. In the crystal structure of CPd8, Lupeol has the highest binding affinity of -6.4. The value of the Positional Root Mean Square Deviation was also computed. VAL2867, THR2864, VAL2899, LYS2903, LYS2906, and LEU2902 are residues located in the receptor's active site. Lupeol, a ligand, may be an effective lung cancer treatment.

Keywords: Lung Cancer, CPd8, Lupeol, Binding affinity, Molecular Docking, and Residues.

Received 12.02.2022

Revised 13.03.2022

Accepted 22.03.2022

INTRODUCTION

Cancer is the second most common cause of death on the globe. Cancer is responsible for around one-sixth of all deaths [1]. Lung cancer is one of the malignancies with a higher death rate than prostate, colon, and breast cancers [2]. Lung cancer is also the second leading cause of new cancer cases in both men and women [3]. Nonsmall cell lung cancer [NSCLC] is a frequent subtype of lung cancer that accounts for 85-90 percent of new cases [4, 5]. Epidermal growth factor [EGFR] overexpression is responsible for about 62 percent of NSCLCs [6]. Chemical medication is now a popular treatment option for NSCLC [7].

Several resistance proteins, including P-GP, lung resistance protein [LRP], and MDR-associated protein, are implicated in the MDR of NSCLC in clinical studies [8, 9]. In lung cancer cells, large levels of LRP expression were seen in the nuclear envelope and cytoplasm [10]. Natural products are becoming increasingly important in the development of next-generation ABC modulators, especially following the dismal outcomes of the first three-generation ABC modulators in clinical trials [11].

In recent years, network pharmacology has emerged as a new science based on system biology and multi-direction pharmacology that can accurately predict drug action mechanisms [12], find new therapeutic targets [13] and better understand the mechanism of interactions between bioactive chemicals and cellular pathways. Molecular docking technology is a useful tool for modernization research since it allows for virtual drug screening [14]. The crystal structure of CPd8 and the Lupeol molecule was docked in the current investigation.

MATERIAL AND METHODS

Protein Preparation

The protein acquired from Protein Data Bank is the most significant molecule for Molecular Docking. The crystal structure of CPd8, an X-Ray diffracted structure with a resolution of 2.84Å [15], was chosen. The undesirable structure in the macromolecule, such as side chains, water molecules, heat atoms, and ligand groups, was eliminated using discovery studio. [Figure1] Then it's saved in PDBQT format for autodock [16].

Ligand Preparation

The docking small molecule or ligand was retrieved from the PubChem database.

Lupeol was found as a three-dimensional structure with the Pub Chem CID 3D 259846 [Figure2]. It was initially saved in SDF format before being converted to PDB format. For autodock compatibility, the energy was reduced and translated to PDBQT format [17].

Docking Protocol

The finest program for molecular docking is Autodock Vina. On autodock vina, the major molecules [protein and ligand] for docking were opened and pre-processed. A grid box with dimensions of 62X58X25 and 72.3995, -18.7200, and 9.81 was produced and centered. The protein and ligand were chosen and the experiment was carried out. The MD's findings were saved in a discovery studio file. Protein and ligand interactions with their molecular surfaces, known as H-bonds, were recorded as PNG files. JPEG files were used to save the 2d interactions and various visualizations of the interactions.

RESULTS AND DISCUSSION

NSCLC has a high malignancy rate, a dismal 5-year survival rate, and a poor prognosis. When compared to chemotherapy, having precise predictive biomarkers and receiving targeted therapy or immunotherapy improves the quality of life and progression-free survival [PFS] for patients with advanced lung cancer [18]. Recently, there has been a surge in interest in using natural substances to treat cancer patients that express P-gp constitutively and are resistant to several chemotherapy drugs. Animals are not poisonous to some of these phytochemicals [19]. These drugs promote the accumulation and efficacy of chemotherapeutic medicines via two possible mechanisms: I functional inhibition of P-GP-mediated transport [20], and/or [ii] a decrease in P-gp expression [21]. One of the main mechanisms of MDR is tumor cells' increased ability to efflux medicines, resulting in a reduction in cellular drug accumulation below dangerous levels. Several members of the ABC superfamily of membrane transporters are involved in active drug efflux [22].

Molecular docking is a structure-based drug design strategy that predicts the affinity and binding pattern of ligands and receptors, speeds up drug design and screening, and provides a foundation for future experimental detection [23]. To investigate the stability and flexibility of ligand-target complexes in a specific system, molecular dynamics simulations are used [24]. As a result, autodock tools were used to undertake molecular docking investigations, and Lupeol was docked with the crystal structure of CPd8 with the PDB ID: 7DN4. Preprocessing of the protein and ligand resulted in an energy minimization of 928.20 for the ligand Gentiobiose. The greatest negative protein binding affinity will be -6.4.

The discovery studio file was used to examine the interactions between proteins and ligands. The distances between H bonds in various aminoacids were computed. VAL2867, THR2864, VAL2899, LYS2903, LYS2906, and LEU2902 are key interacting residues. [Table 1] shows the distances between H-bonds and the H-bond interacting residues. The root means square deviation value will be zero in those conformations. [Table 2] shows the binding affinity of those compounds with the macromolecule in various conformations, as well as the Root Mean Square Deviation [RMSD] values of the interacting molecules [Protein and Ligand]. [Figures 3, 4, 5, 6, 7and 8] show the interactions of protein and ligand [Lupeol]. It's also visible in charts like the Ramachandran plot [Figure 9], the Hydrophobicity plot [Figure 10], and contact plots like the CAlpha plot [Figure 11], the CBeta plot [Figure 12], the Sidechain plot [Figure 13], the H bond plot [Figure 14], and the Residue plot [Figure 15]. As a result, molecular docking simulation ligand-target binding, as well as mechanism study on Lupeol therapy for NSCLC, may serve as a platform for future NSCLC targeted medication development.

Table 1. The molecular docking studies of compounds with the crystal structure of CPd8

S. No	Compound name	Docking score	H-Bond Interaction	Distance
1.	Lupeol	-6.4	VAL2867	3.81
				4.66
			THR2864	4.61
				4.95
				2.87
				2.59
			VAL2899	4.55
				4.66
				4.24
			LYS2903	4.23
				4.27
				5.16
			LYS2906	4.75
				4.89
	4.19			
	LEU2902			

Table 2 shows the various binding affinity and root mean square deviation [RMSD] Upper and Lower Bound values of Lupeol

Ligand	Binding Affinity	rmsd/ub	rmsd/lb
pro7dn4_A_Lupeol_uff_E=928.20	-6.4	0	0
	-6.3	22.112	19.457
	-6.3	27.735	22.741
	-6.2	19.255	16.35
	-6	25.263	21.046
	-5.9	23.696	19.884
	-5.9	23.113	20.91
	-5.9	25.153	22.376
	-5.8	23.462	20.093

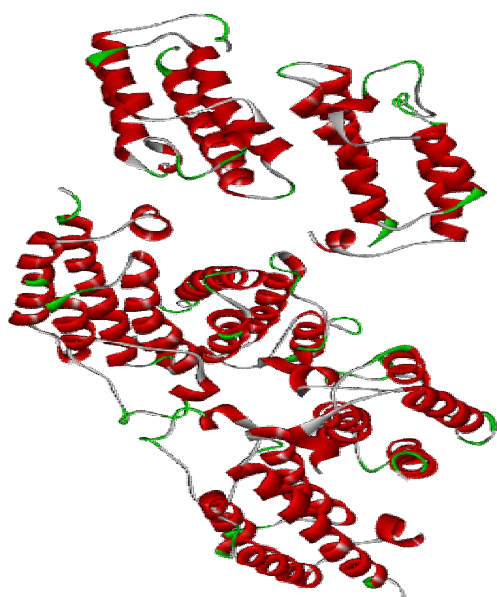


Figure 1 shows 3d structure of crystal structure of CPd8

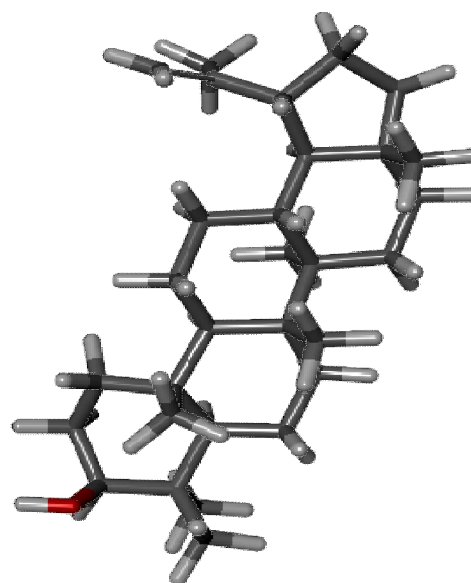


Figure 2 shows the 3d structure of Lupeol

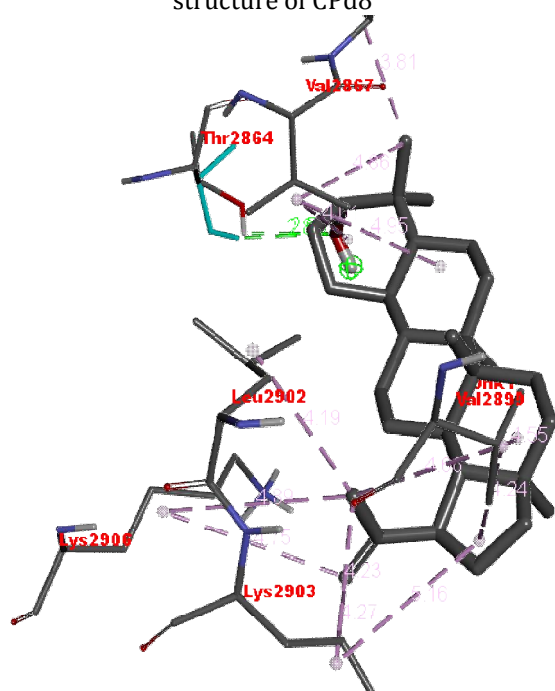


Figure 3 shows the interaction of Lupeol with the crystal structure of CPd8

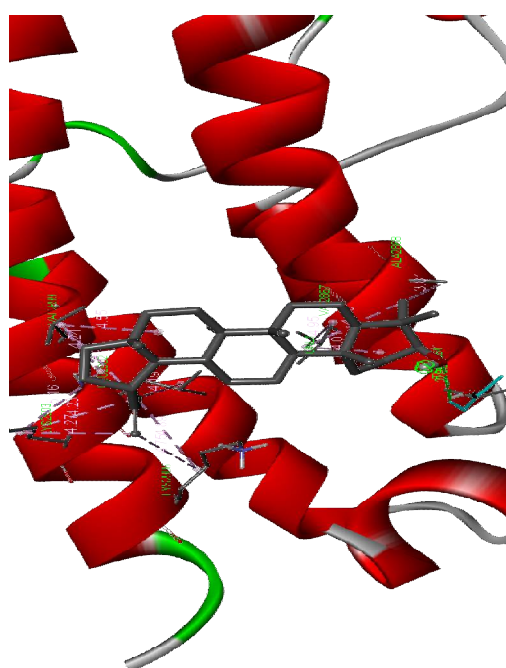


Figure 4 shows the interaction of Lupeol with the crystal structure of CPd8 with a receptor

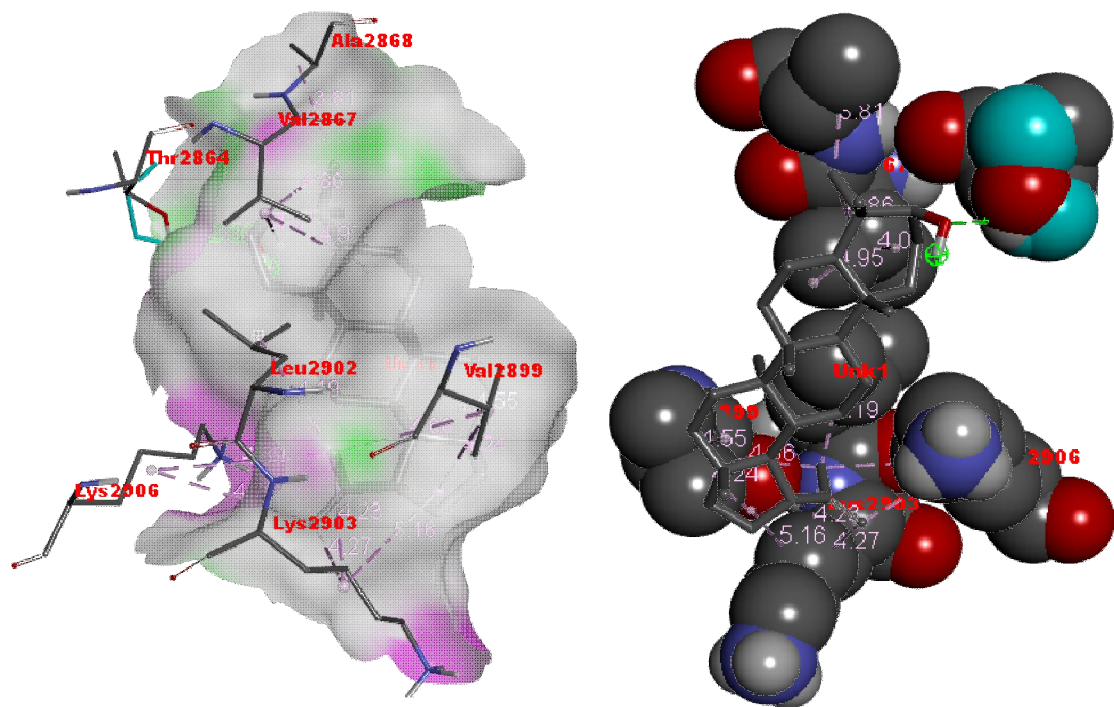


Figure 5,6 shows the interaction of Lupeol with the crystal structure of CPd8

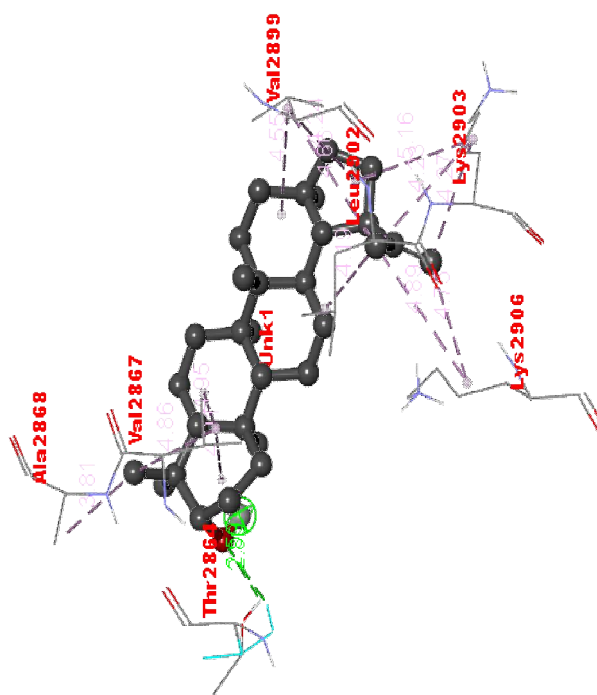


Figure 7 shows the interaction of Lupeol with the crystal structure of CPd8

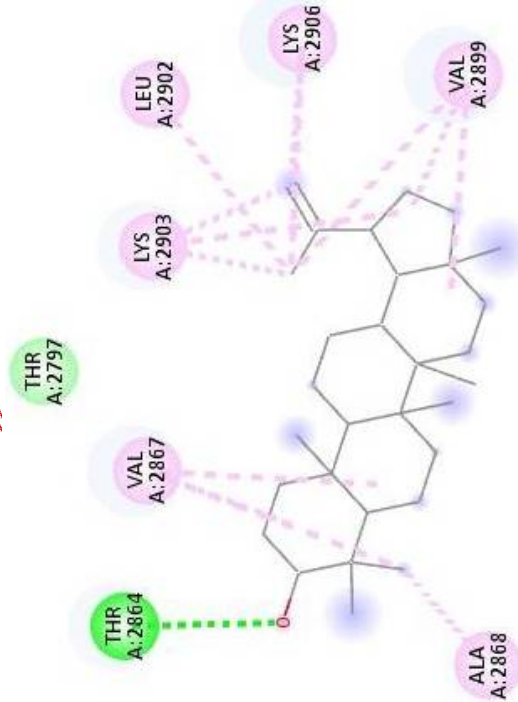


Figure 8 shows the 2d diagram of the interaction of Lupeol with the crystal structure of CPd8

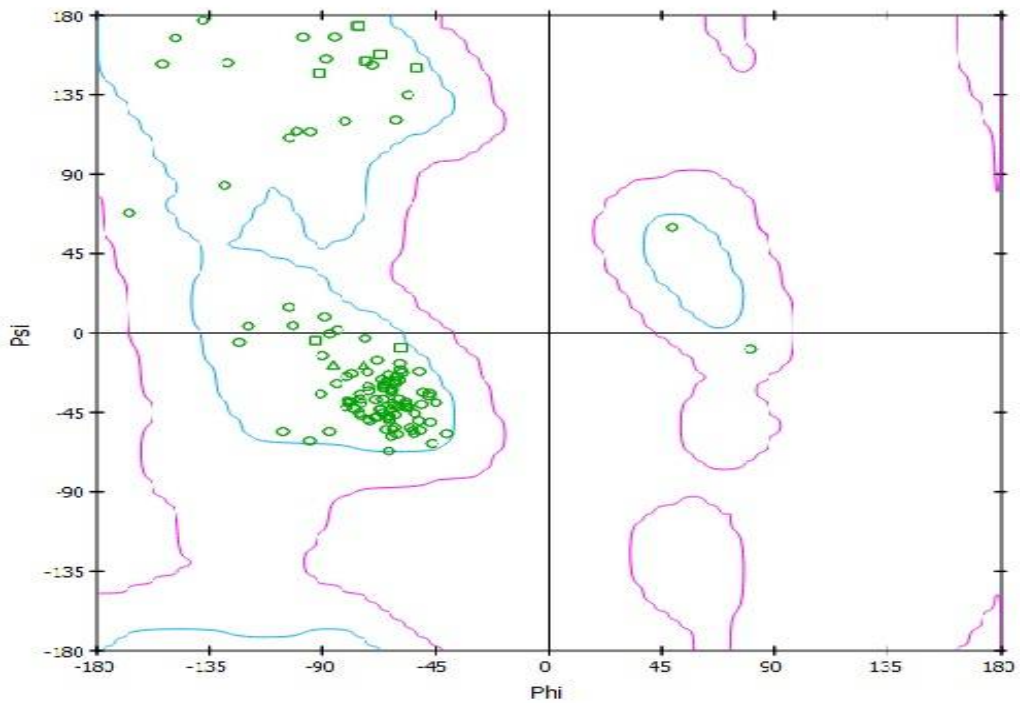


Figure 9 shows the interaction of Lupeol with the crystal structure of CPd8 in Ramachandran Plot

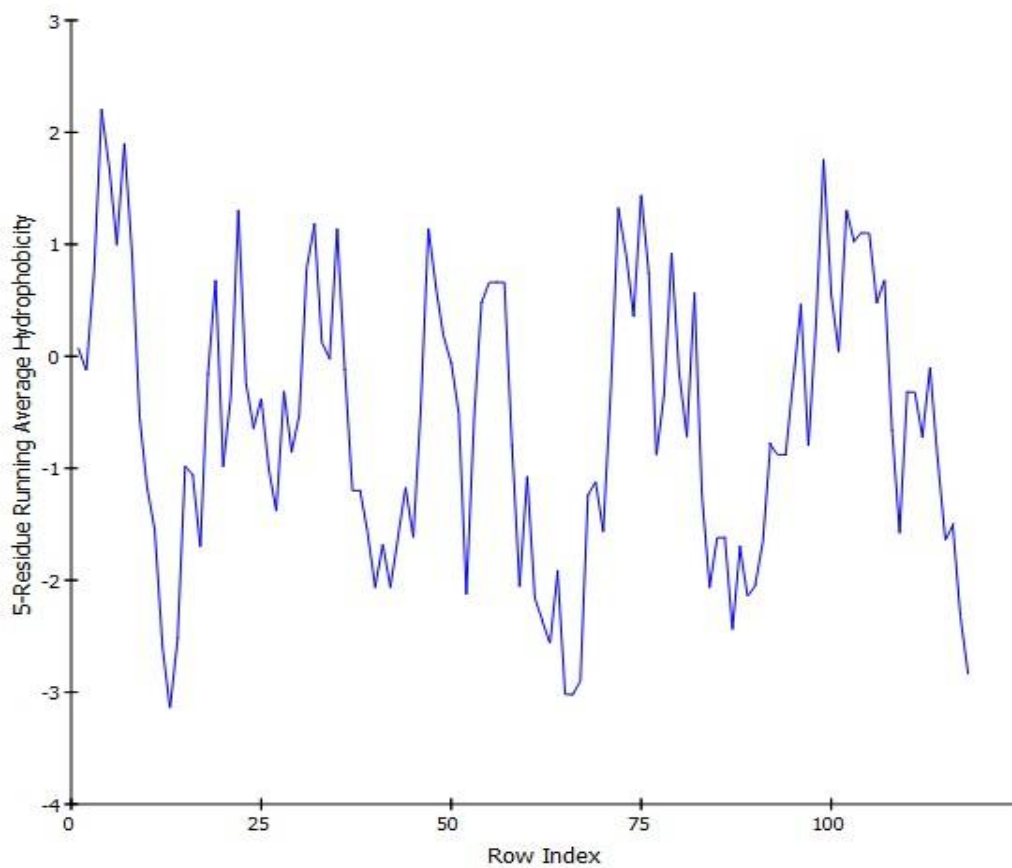


Figure 10 shows the interaction of Lupeol with the crystal structure of CPd8 in Hydrophobicity Plot

complex1:CApha

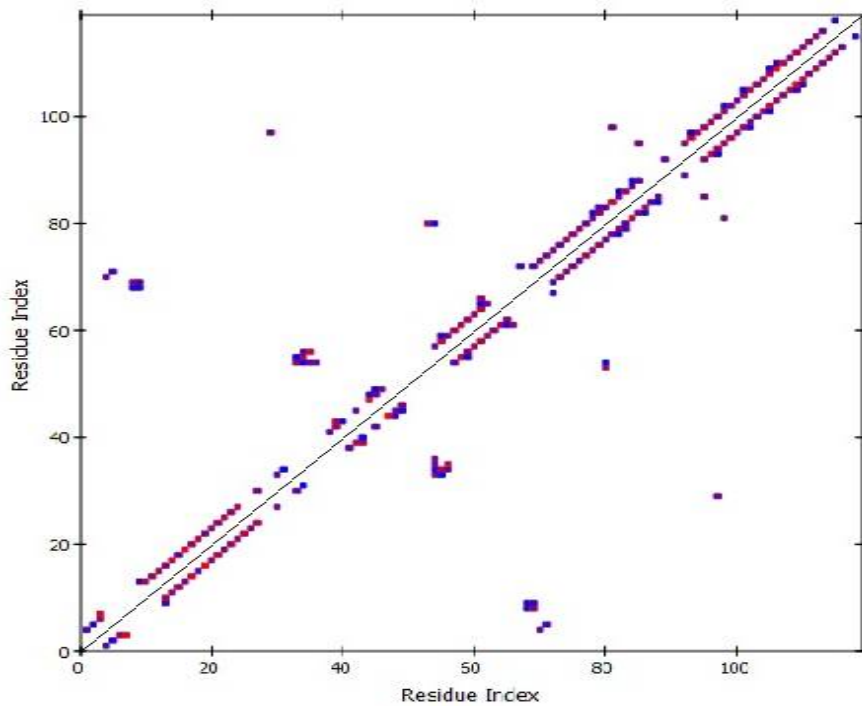


Figure 11 shows the interaction of Lupeol with the crystal structure of CPd8 in C-Alpha Plot

complex1:CBeta

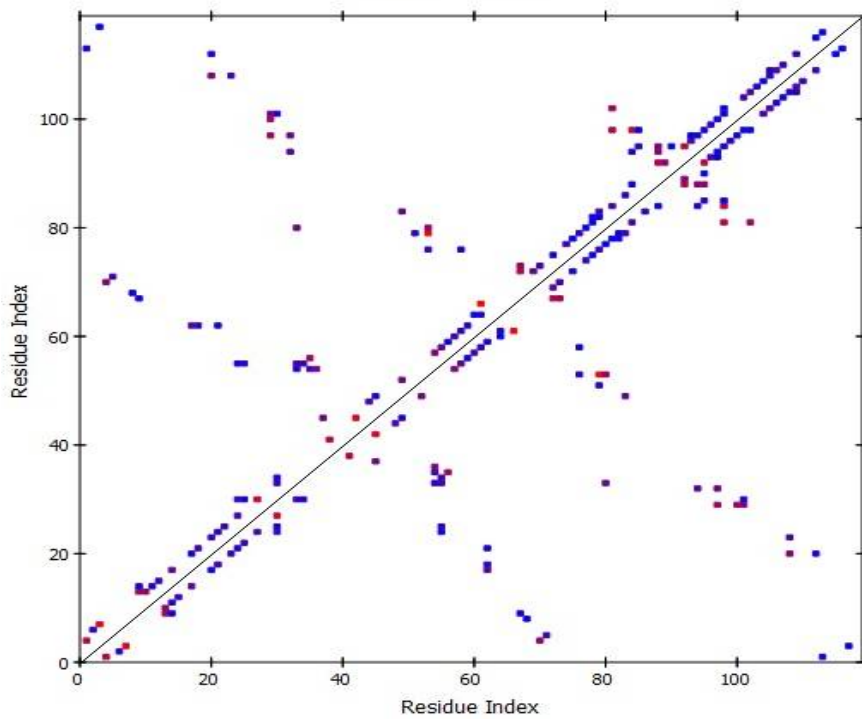


Figure 12 shows the interaction of Lupeol with the crystal structure of CPd8 in C-Beta Plot

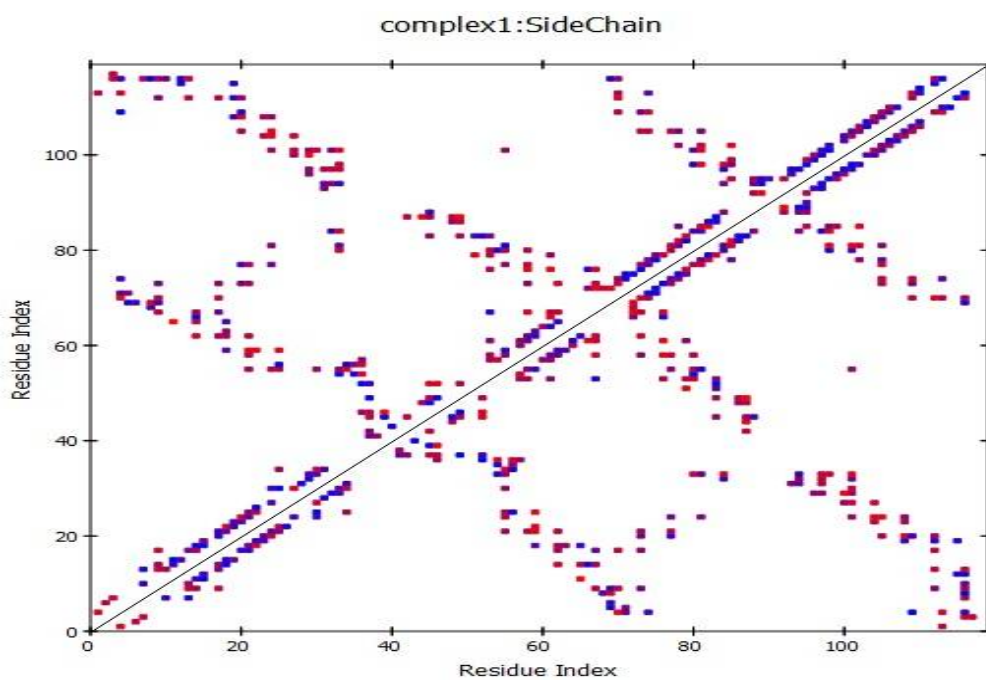


Figure 13 shows the interaction of Lupeol with the crystal structure of CPd8 in Sidechain Plot

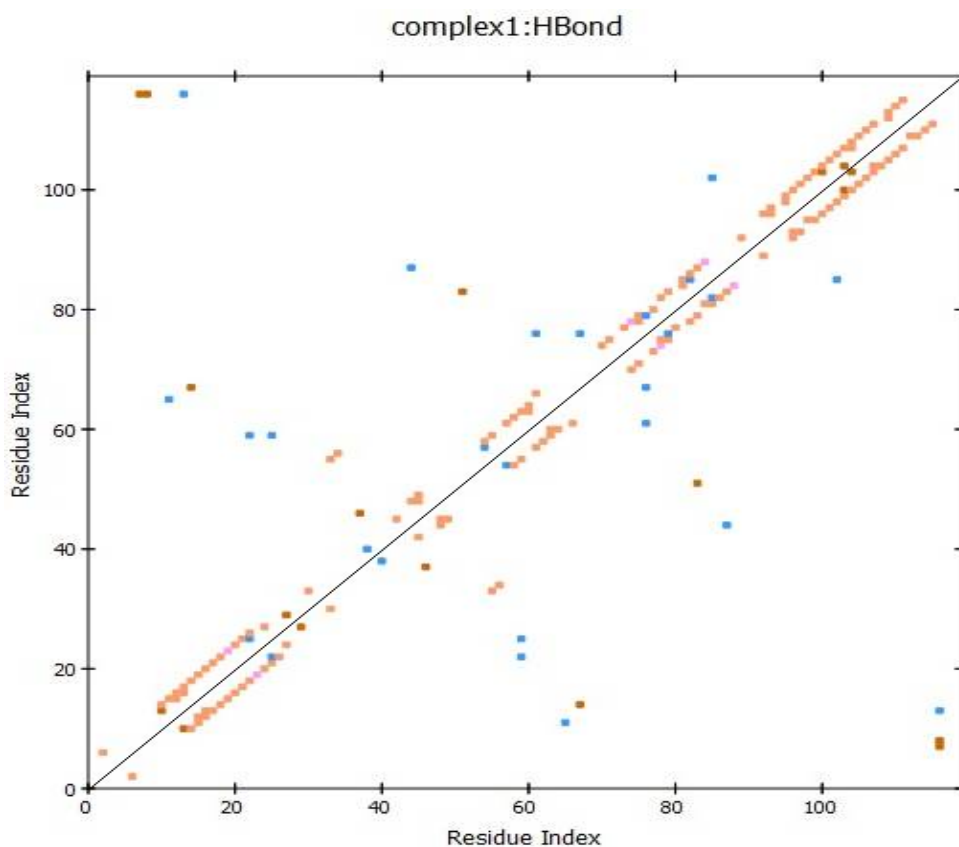


Figure 14 shows the interaction of Lupeol with the crystal structure of CPd8 in H-bond Plot

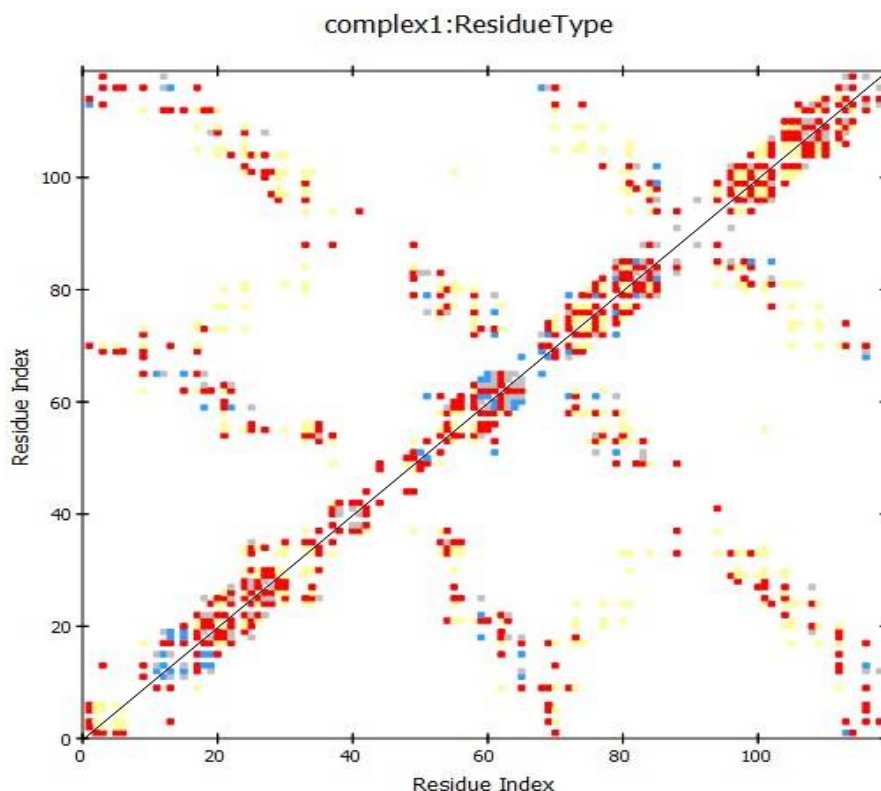


Figure 15 shows the interaction of Lupeol with the crystal structure of CPd8 in Residue Plot

CONCLUSION

Even though there are numerous treatments for lung cancer, the development of effective therapy is critical due to the high death rate. As a result, computational analyses of the crystal structures of CPd8 and Lupeol were conducted. With 15 interactions, the greatest binding score is -6.4. Literature and different graphs also support the receptor-ligand relationships. VAL2867, THR2864, VAL2899, LYS2903, LYS2906, and LEU2902 are the residues identified in the receptor's binding site. As a result, Lupeol has the potential to be a cure for lung cancer.

ACKNOWLEDGEMENT

For Docking Studies, the authors gratefully acknowledge the Department of Botany, Srimad Andavan Arts and Science College [Autonomous], Tiruchirapalli-620005, Tamil Nadu, India.

REFERENCES

- Ji, B. S., He, L., & Liu, G. Q. (2005). Reversal of p-glycoprotein-mediated multidrug resistance by CJX1, an amlodipine derivative, in doxorubicin-resistant human myelogenous leukemia (K562/DOX) cells. *Life sciences*, 77(18), 2221-2232.
- Saikia, S., & Bordoloi, M. (2019). Molecular docking: challenges, advances and its use in drug discovery perspective. *Current drug targets*, 20(5), 501-521.
- Tang, X. Q., Bi, H., Feng, J. Q., & Cao, J. G. (2005). Effect of curcumin on multidrug resistance in resistant human gastric carcinoma cell line SGC7901/VCR. *Acta Pharmacologica Sinica*, 26(8), 1009-1016.
- Anuchapreeda, S., Leechanachai, P., Smith, M. M., Ambudkar, S. V., & Limtrakul, P. N. (2002). Modulation of P-glycoprotein expression and function by curcumin in multidrug-resistant human KB cells. *Biochemical pharmacology*, 64(4), 573-582.
- Limtrakul, P., Khantamat, O., & Pintha, K. (2004). Inhibition of P-glycoprotein activity and reversal of cancer multidrug resistance by *Momordica charantia* extract. *Cancer chemotherapy and pharmacology*, 54(6), 525-530.
- Binkowski, T. A., Naghibzadeh, S., & Liang, J. (2003). CASTp: computed atlas of surface topography of proteins. *Nucleic acids research*, 31(13), 3352-3355.
- Morris, G. M., Goodsell, D. S., Halliday, R. S., Huey, R., Hart, W. E., Belew, R. K., & Olson, A. J. (1998). Automated docking using a Lamarckian genetic algorithm and an empirical binding free energy function. *Journal of computational chemistry*, 19(14), 1639-1662.
- Sparreboom, A., Danesi, R., Ando, Y., Chan, J., & Figg, W. D. (2003). Pharmacogenomics of ABC transporters and its role in cancer chemotherapy. *Drug Resistance Updates*, 6(2), 71-84.

9. Amalia, I. F., Sayyidah, A., Larasati, K. A., & Budiarti, S. F. (2020). Molecular Docking Analysis of α -Tomatine and Tomatidine to Inhibit Epidermal Growth Factor Receptor (EGFR) Activation in Non-Small-Cell Lung Cancer (NSCLC). *JSMARTech: Journal of Smart Bioprospecting and Technology*, 2(1), 1-6.
10. Koperuncholan, M., & Ahmed John, S. (2011). Biosynthesis of Silver and Gold Nanoparticles and Antimicrobial Studies of Some Ethno medicinal Plants in South-Eastern Slope of Western Ghats. *IJPI'S Journal of Pharmacognosy and Herbal Formulations*, 1(5), 10-15.
11. Koperuncholan, M., & John, S. A. (2011). Antimicrobial and Phytochemical Screening in *Myristica dactyloides* Gaertn. *Journal of Pharmacy Research*, 4(2), 398-400.
12. Fazal Mohamed, M. I., Arunadevi, S., Koperuncholan, M., & Mubarak, M. S. (2011). Synthesis and antimicrobial activity of some naphthyl ether derivatives. *De r Chemica Sinica*, 2, 52-57.
13. Koperuncholan, M. (2015). Bioreduction of chloroauric acid (HAuCl₄) for the synthesis of gold nanoparticles (GNPs): a special emphathies of pharmacological activity. *Int. J. Phytopharm*, 5(4), 72-80.
14. Ahmed John, S., & Koperuncholan, M. (2012). Direct root regeneration and indirect organogenesis in *Silybum marianum* and preliminary phytochemical, antibacterial studies of its callus. *The International Journal of Pharmaceutics*, 2, 52-57.
15. Koperuncholan, M., & Manogaran, M. (2015). Edible plant-mediated biosynthesis of silver and gold nanoflakes against human pathogens. *World Journal of Pharmaceutical Research*, 4(1), 1757-1775.
16. Sinthiya, A., & Koperuncholan, M. (2015). In-silico characterization for Multiple sclerosis: A special emphasis on Tetrakis (4-aminopyridine-kN1) dichloridocopper (II) monohydrate with sphingosine 1phosphate lyase. *Crystal Research*, 89, 36824-36826.
17. Baskaran, T., Kandavel, D., & Koperuncholan, M. (2018). Investigation of trace metals and secondary metabolites from *Pavetta indica* and study their antimicrobial efficacy. *Research Directions*, 6(6), 273-282.
18. Sinthiya, A., & Koperuncholan, M. (2019). Synthesis and characterization of l-amino acid doped 2-aminopyridine co-crystals for anti-cancer activity. *Life Science Informatics Publications-Research Journal of Life Sciences, Bioinformatics, Pharmaceutical, and Chemical Sciences*, 5(2), 754-762.
19. John, S. A., & Koperuncholan, M. (2012). Antibacterial Activities of various solvent extracts from *Impatiens balsamina*. *International Journal of pharma and biosciences*, 3(2), 401-406.
20. Koperuncholan, M., Sathish Kumar, P., Sathyanarayanan, G., & Vivek, G. (2010). Phytochemical Screening and Antimicrobial Studies of Some Ethnomedicinal Plants in South-Eastern Slope of Western Ghats. *Int. J. Med. Res*, 1, 48-58.
21. Harinee, S., Muthukumar, K., Dahms, H. U., Koperuncholan, M., Vignesh, S., Banu, R. J., & James, R. A. (2019). Biocompatible nanoparticles with enhanced photocatalytic and anti-microfouling potential. *International Biodeterioration & Biodegradation*, 145, 104790.
22. Santhakumar, M., & Koperuncholan, M. (2019). Gold nano-drug design for antimicrobial activity. *Life Science Informatics Publications-Research Journal of Life Sciences, Bioinformatics, Pharmaceutical, and Chemical Sciences*, 5(2), 720-731.
23. Ramesh, T., Koperuncholan, M., Praveena, R., Ganeshkumari, K., Vanithamani, J., Muruganantham, P., & Renganathan, P. (2019). Medicinal properties of some *Dendrobium* orchids-A review. *Journal of Applied and Advanced Research*, 4(4), 119-128.
24. Ramesh, V., Ahmed John, S., & Koperuncholan, M. (2014). Impact of cement industries dust on selective green plants: a case study in ariyalur industrial zone. *International Journal of Pharmaceutical, Chemical & Biological Sciences*, 4(1). 152-158.

CITATION OF THIS ARTICLE

T Baskaran, D Kandavel, V Aravindha, M Koperuncholan. Computational Modelling of Lung Cancer Treats with Lupeol. *Bull. Env. Pharmacol. Life Sci.*, Vol11 [4] March 2022 : 30-38.